ELSEVIER

Applied Surface Science 197–198 (2002) 107–113

applied surface science

www.elsevier.com/locate/apsusc

Theoretical description of the ultrafast ablation of diamond and graphite: dependence of thresholds on pulse duration

Harald O. Jeschke*, Martin E. Garcia

Institute for Theoretical Physics, Freie Universität Berlin, Arnimallee 14, 14195 Berlin, Germany

Abstract

A theoretical description of the ultrafast ablation of diamond and graphite is presented. Laser induced lattice deformations and melting are described with the help of molecular dynamics simulations on time dependent potential energy surfaces derived from a microscopic electronic Hamiltonian. Thermalization effects are explicitly taken into account. We calculate the ablation thresholds as a function of the pulse duration for femtosecond pulses. For both materials we obtain smoothly increasing thresholds for increasing duration. The damage and ablation mechanisms are discussed.

Keywords: Ultrafast ablation; Dependence of thresholds; Pulse duration

1. Introduction

The irradiation of solids with femtosecond lasers leads to interesting ultrafast phenomena, for example, ultrafast phase transitions [1–12], ablation [13–15], excitation of coherent phonons [16], and optical breakdown [17].

In particular, and due to its important technological applications [18], ultrafast laser ablation has been extensively studied.

The ablation threshold refers to the laser fluence for which lattice instabilities of such magnitude are induced that the material undergoes an irreversible damage and at least a monolayer of material is removed [19].

It is now well established, that the subpicosecond laser pulses induce in the irradiated materials effects which qualitatively differ from those produced by long pulses with durations of several tens of pico-or nanoseconds. Therefore, the ablation processes yield different results depending on which kind of laser pulse is used to irradiate the material.

However, little is known about the quantitative differences of the thresholds for different pulse durations within the sub-picosecond domain. In this paper, we perform a theoretical study of the dependence of ablation and damage thresholds on pulse duration for femtosecond laser pulses with durations between 5 and 500 fs. In particular, we analyze the laser excitation of graphite and diamond.

Most of the experimental investigations performed so far suggest that the ablation process near the threshold is always initiated by the ultrafast melting of the material. Recently, it has been shown that there is an exception to this rule: due to its layered, sp^2-bonded structure, graphite presents the unique property of exhibiting two different ablation mechanisms, and therefore two different ablation thresholds. The mechanism for the low fluence ablation threshold

* Corresponding author. Fax: +49-30-838-56799.
E-mail address: jeschke@physik.fu-berlin.de (H.O. Jeschke).

0169-4332/02/$ – see front matter
PII: S0169-4332(02)00312-4

is the removal of intact graphite sheets and does not involve melting [9]. In contrast, the high fluence threshold corresponds to bond breaking processes inside the graphite layers and leads to ultrafast melting and expansion of the system, the intermediate liquid state induced by the laser showing signatures corresponding to low density liquid carbon (LDLC) [9].

As a matter of fact, not only for graphite but also in the case of the laser excitation of diamond one can define at least two different thresholds. At high fluences the typical ablation involving removal of material occurs, whereas for lower fluences a nonequilibrium graphitization takes place [7,8]. Throughout this paper, we will refer to the low fluence thresholds simply as damage threshold.

2. Theory

Our approach is based on the following physical picture [7]. The laser pulse excites electrons from occupied to unoccupied levels with a time-dependent probability which is proportional to the intensity of the laser field. As a consequence of this extremely fast excitation process, a nonequilibrium distribution of electrons is created. This nonequilibrium state converges rapidly, through electron–electron collisions, to an equilibrium (Fermi-like) occupation of the electronic levels. In addition, a diffusion process from the excited region into the rest of the material sets in. During this complex electron dynamics the atoms undergo a relaxation process due to the dramatic changes in the potential energy surface (PES). This atomic motion may lead, depending on the intensity of the laser pulse, to structural changes, ultrafast melting of ultrafast ablation.

From the earlier discussion, it is clear that a description of laser induced nonequilibrium structural phase transitions requires taking into account as many atomic degrees of freedom as possible.

Our study concentrates on a subregion in the center of the irradiated area, which can change its structure, form and volume rapidly. In this way, and in contrast to the case of constant volume, part of the energy pumped into the system by the laser pulse is spent for expansion or deformation, preventing ultrafast melting [7,8]. Furthermore, the system is allowed to explore new lattice structures, which are unavailable if the volume is kept constant. The only constraint on the system is that the external pressure remains constant.

Thus, we employ an MD technique proposed by Parrinello and Rahman [20] which is based upon a Lagrangian of the form

$$L(t) = \sum_{i=1}^{N} \tfrac{1}{2} m_i \dot{\boldsymbol{s}}_i^{\mathrm{T}} h^{\mathrm{T}} h \dot{\boldsymbol{s}}_i - \Phi(\{r_{ij}\}, t) + K - P\Omega. \tag{1}$$

Here, the coordinates $\dot{\boldsymbol{s}}_i$ of the N atoms are taken relative to the vectors $\boldsymbol{a}$, $\boldsymbol{b}$ and $\boldsymbol{c}$ that form the MD supercell. These primitive vectors form the columns of the matrix $h = (\boldsymbol{a}\,\boldsymbol{b}\,\boldsymbol{c})$. The absolute coordinates of the atoms are given by $\boldsymbol{r}_i = h\boldsymbol{s}_i$. Here, $\Omega = \det(h)$ is the volume of the MD supercell, P the external pressure. The second term represents the PES, which is determined from a microscopic theory as described later. The first two terms of the Lagrangian would lead to the usual Newton equations of motion, while the third and fourth terms are introduced to simulate the time evolution of the MD unit cell, the coordinates of which are considered as 9 extra degrees of freedom. The third term $K = (W/2)\mathrm{Tr}(\dot{h}^{\mathrm{T}}\dot{h})$ describes the kinetic energy of the MD supercell, W the a parameter with the dimension of mass.

Using the Euler–Lagrange formalism, $N + 9$ equations of motion for the atomic coordinates $\boldsymbol{s}_i$ and for the MD cell coordinates h_{kl} are derived from Eq. (1).

The PES is determined by $\Phi(\{r_{ij}\}, t) = \sum_m n(\varepsilon_m, t)\varepsilon_m(\boldsymbol{r}_1, \ldots, \boldsymbol{r}_N) + E_{\mathrm{rep}}(\{r_{ij}\})$, where $E_{\mathrm{rep}}(\boldsymbol{r}_1, \ldots, \boldsymbol{r}_N)$ contains the repulsive interactions between the atomic cores, and ε_m are the eigenvalues of the Hamiltonian

$$H = \sum_{i\alpha} \epsilon_{i\alpha} n_{i\alpha} + \sum_{\substack{ij\alpha\beta \\ j\neq i}} V_{ij}^{\alpha\beta}(r_{ij}) c_{i\alpha}^{+} c_{j\beta}. \tag{2}$$

Here, $\epsilon_{i\alpha}$ is the on-site energy of atom i and orbital α. The $c_{i\alpha}^{+}$ and $c_{j\beta}$ are the creation and annihilation operators, and $V_{ij}^{\alpha\beta}(r_{ij})$ the hopping integrals. For the description of carbon, the 2s, $2p_x$, $2p_y$ and $2p_z$ orbitals are taken into account. For the radial part of the hopping integrals and for E_{rep}, we employ the forms proposed by Xu et al. (For more details see [21]).

The forces which enter the equations of motion as $\mathrm{d}\Phi(r_{ij})/\mathrm{d}\boldsymbol{s}_k$ are determined using the Born–Oppenheimer approximation and are given by

$$\boldsymbol{f}_i = -\sum_m n(\varepsilon_m, t)\left\langle m\left|\frac{\partial H}{\partial \boldsymbol{s}_i}\right|m\right\rangle - \frac{\partial E_{\mathrm{rep}}}{\partial \boldsymbol{s}_i}, \tag{3}$$

where m labels the electronic levels, which are the eigenstates of the electronic Hamiltonian $H(\boldsymbol{r}_1, \ldots, \boldsymbol{r}_N)$. For the derivation of Eq. (3), the Hellmann–Feynman theorem has been used. The forces for the MD supercell h result in close analogy. In Eq. (3), $n(\varepsilon_m, t)$ refers to the occupation of the energy level ε_m at time t. This time-dependent occupation changes due to the action of the laser pulse, Coulomb interactions and diffusion effects. The occupation $n(\varepsilon_m, t)$ is initially given by a Fermi distribution at the temperature of the lattice. During the excitation by the laser pulse, this distribution changes in time according to [7,9]

$$\begin{aligned}\frac{\mathrm{d}n(\varepsilon_m, t)}{\mathrm{d}t} = &\int_{-\infty}^{\infty} \mathrm{d}\omega\, g(\omega, t-\tau)\{[n(\varepsilon_m - \hbar\omega, t-\tau) \\ &+ n(\varepsilon_m + \hbar\omega, t-\tau) - 2n(\varepsilon_m, t-\tau)]\} \\ &- \frac{n(\varepsilon_m, t) - n^0(\varepsilon_m)}{\tau_1}.\end{aligned} \tag{4}$$

Here, the first term describes the laser induced excitation processes $\varepsilon_m \rightarrow \varepsilon_m \pm \hbar\omega$ which are weighted by the spectral function $g(\omega, t)$ of the laser pulse at each time step τ. The second term of Eq. (4) takes into account, in a simple approximation, the thermalization processes due to electron–electron collisions. The nonequilibrium distribution $n_{\varepsilon_m}(t)$ relaxes towards a Fermi distribution $n^0(\varepsilon_m) = 2/\{\exp[(\varepsilon_m - \mu)/k_B T_e(t)] + 1\}$ with a (energy-independent) time constant τ_1.

At the short time scale of a few picoseconds, the main process causing dissipation of the absorbed energy is the diffusion of hot electrons into the surrounding cold lattice. This is taken into account by a further rate equation [7].

3. Results

In this section, we present results for damage and ablation thresholds of diamond and graphite. The thresholds have been calculated for a constant external pressure of $p = 10^5$ Pa. All trajectories were calculated for an MD supercell of $N = 64$ atoms.

The laser excitation of graphite and diamond was studied for different pulse durations and laser intensities. We considered laser pulses of Gaussian shape and duration τ between 5 and 500 fs. Since the energy absorbed by graphite and diamond shows a complicated dependence on the laser intensity [22], we present our results in terms of the absorbed energy, which is a more relevant quantity than the peak intensity of the Gaussian pulse. We show below how to determine the laser fluences which lead to the absorbed energies obtained in our calculations.

In Fig. 1 , we present the damage and ablation thresholds of diamond as a function of laser pulse duration. The two thresholds are identified as follows. For absorbed energies below the damage threshold, there is no change of the structure of the material. The electron-hole plasma has a density lower than $\xi = 2\%$ and causes only a slight increase of the lattice temperature. For increasing absorbed energies, bond breaking processes start to be important, and structural changes can take place. Above the damage threshold we observe an ultrafast structural change, consisting in the formation of graphite layers. This laser induced ultrafast phase transition, discussed in detail in [7,8], can be briefly described as the following collective motion of the atoms. First, the bent hexagons of the diamond lattice in the (1 1 0) direction break up to form planes. In addition, in the direction perpendicular to the newly formed planes, the originally bent hexagons become flat and form the hexagons of the graphite lattice. While for the damage threshold, no clear dependence on the pulse duration may be observed, the ablation threshold shows a slight increase from an absorbed energy of $E_0 = 3.7$ eV per atom for pulses of $\tau = 20$ fs to $E_0 = 5.0$ eV per atom for $\tau = 500$ fs.

Between the damage and ablation thresholds, the structure of the material is modified. For the determination of this intermediate region it is important that the laser energy is not high enough to destroy the cohesion of the lattice completely. However, above the ablation threshold the electron-hole plasma of a density larger than $\xi = 14\%$ created by the pulse leads to a very fast evaporation of the material. As a result a gas of carbon monomers and small fragments of carbon chains are formed. Note, the present theory is not well suited for the determination of the dynamics far above the ablation threshold, since it does not describe ablation

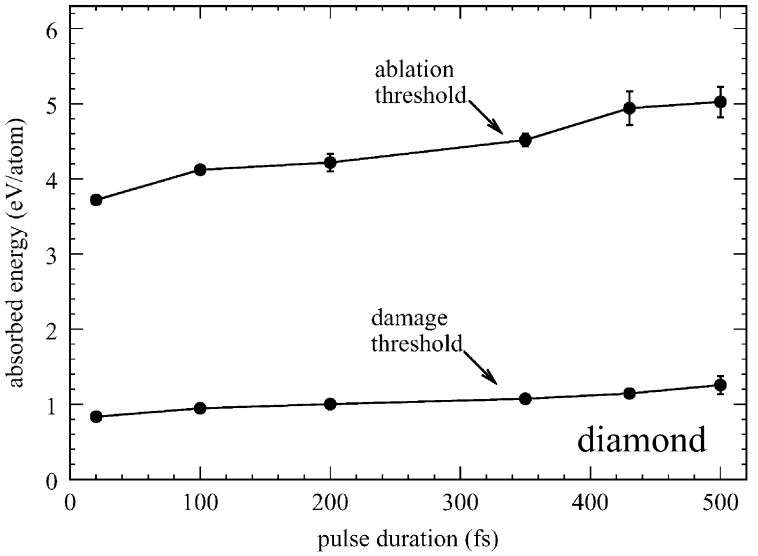

Fig. 1. Damage and ablation thresholds of diamond as a function of laser pulse duration. Trajectories were calculated for an $N = 64$ atom MD supercell.

mechanisms including ionization and Coulomb explosion. The mechanism that leads to ablation here is the excitation of a large number of valence electrons into anti-bonding states. This produces a strong change in the PES. Due to the resultant repulsion the crystal lattice becomes instable.

In Fig. 2, we show the ablation threshold for graphite as a function of pulse duration. As in the case of diamond the ablation is defined as an evaporation of the material. Below the ablation threshold interesting structural changes occur and Fig. 2 shows a damage threshold that is approximately 1 eV lower

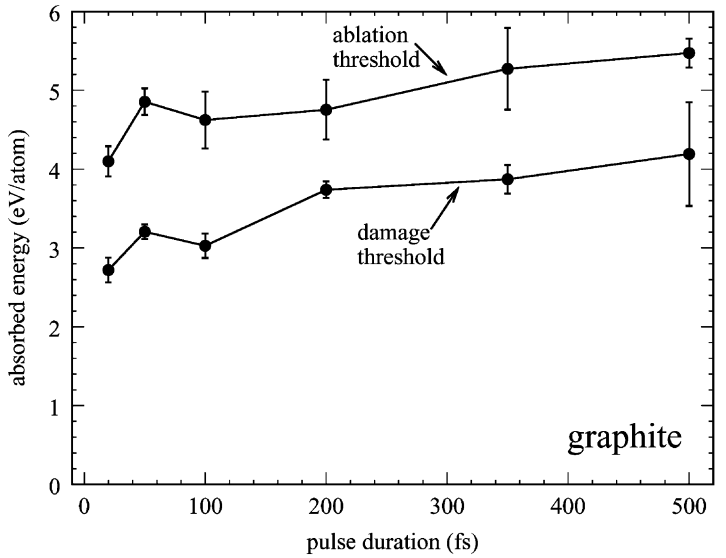

Fig. 2. Damage and ablation thresholds of diamond as a function of laser pulse duration. Trajectories were calculated for a $N = 64$ atom MD supercell.

in energy than the ablation threshold. Calculation with a much higher number of atoms ($N = 576$) in a film geometry confirmed that in fact a second ablation threshold below the one presented in Fig. 2 can be distinguished [9]. It includes a strong vibrational excitation of the graphite planes. These remain intact, but they collide because of the strong oscillation of the atoms perpendicular to the planes and then, ablation of entire planes can occur as a consequence of the momentum transferred in these collisions [9]. These oscillations correspond both to phonons and to anharmonic motions excited by the laser which die out quickly as electron and lattice temperatures equilibrate.

Both thresholds shown in Fig. 2 increase very slightly with pulse duration, but this effect is not very pronounced.

We can compare the order of magnitude of the calculated damage thresholds of diamond and graphite with the experiment of Downer and co-workers [5]. With $\lambda = 620$ nm laser pulses of $\tau = 90$ fs duration they find damage in HOPG above the fluence $F_m = 0.13 \pm 0.02$ J/cm^2 and in diamond above $F_m = 0.63 \pm 0.15$ J/cm^2. For comparison with absorbed energies E_0 in eV per atom, we can estimate a theoretical value for the fluence as

$$F = \frac{e\,E_0\,n_\mathrm{a}\,d}{1 - R - T}\,, \tag{5}$$

where e is the Coulomb constant, n_a the atomic density, d the penetration depth of the light, R the reflectivity and T the transmission of the material. Assuming one-photon absorption for the penetration depth, we use $d = \lambda/4\pi k$ [23] where λ is the wavelength and k the extinction coefficient. Thus, for $\lambda = 620$ nm, we find $d = 330$ Å in graphite ($k = 1.5$ [5]) and $d = 770$ Å in diamond (with $k = 0.64$ calculated from $R = 0.2$ and the refractive index $n = 2.42$). A damage threshold of $E_0 = 3$ eV per atom in graphite at $\tau = 100$ fs (see Fig. 2) then corresponds to $F = 0.26$ J/cm^2 (with $n_\mathrm{a} = 1.14 \times 10^{23}$ atoms/cm^3, $R = 0.3$ [5], $T = 0$). A damage threshold of $E_0 = 1$ eV per atom in diamond at $\tau = 100$ fs (see Fig. 1) corresponds to $F = 1.2$ J/cm^2 (with $n_\mathrm{a} = 1.76 \times 10^{23}$ atoms/cm^3, $R = 0.17$, $T = 0.65$ [5]). Thus, we find theoretical values for the damage thresholds which are larger than the experimental values but which are of the correct order of magnitude. Considering that we have made a very rough estimate for the penetration depth of the light (no two- and three-photon absorption coefficients were available) this result is acceptable.

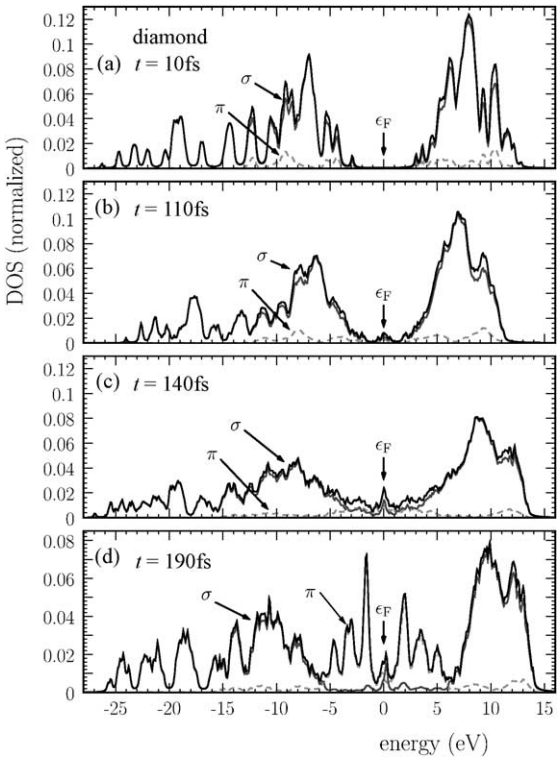

Fig. 3. DOS during a nonequilibrium graphitization of diamond. The time is given with respect to the peak of a laser pulse of $\tau = 20$ fs duration. The π contribution to the DOS is indicated by a dashed line. Note, the ordinate scale of (d) has been changed with respect to (a)–(c). For a detailed description of the changes to the DOS see the text.

In Fig. 3, we show the densities of states (DOS) corresponding to the ultrafast graphitization process (i.e. above the damage threshold). In addition to the total DOS, σ and π contributions are shown. At a time $t = 10$ fs (see Fig. 3(a)), measured from the maximum of the laser pulse of $\tau = 20$ fs duration, the DOS is still that of intact diamond with a very small π contribution and a gap of $E_g = 5.5$ eV. At $t = 110$ fs (see Fig. 3(b)), the structures of diamond DOS are broadening, and we see the emergence of a small number of states in the gap. At $t = 140$ fs (see Fig. 3(c)), the structures of the diamond DOS have broadened even further, and close to the Fermi level, the density is increasing.

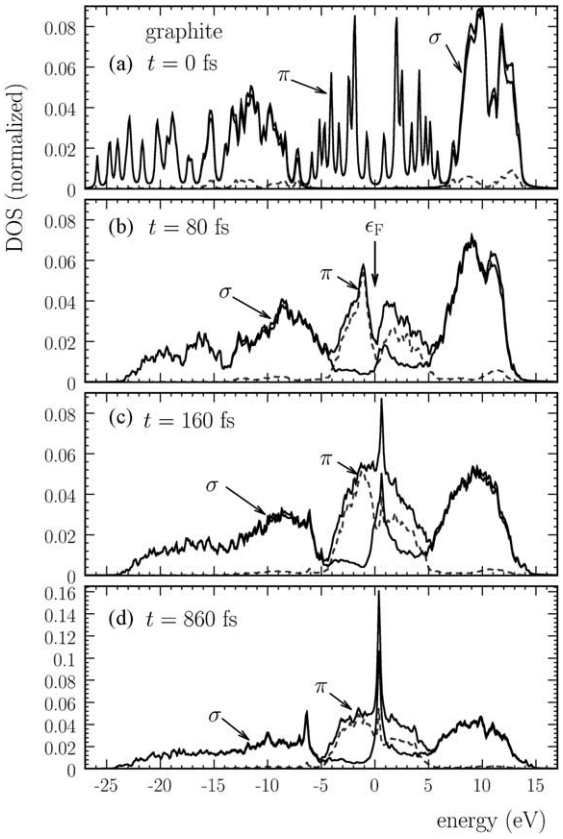

Fig. 4. DOS for the ablation of graphite at an absorbed energy of $E_0 = 4.0$ eV per atom. The π contribution to the DOS is indicated by a dashed line. The features of the graphite DOS in (a) at $t = 0$ fs are quickly replaced by a metallic-like DOS (b). The sharp peak at the Fermi level that appears at $t = 160$ fs in (c) is due to contributions of linear carbon chains. Note, the ordinate scale of (d) is different from (a) to (c).

This increase is to a large part due to π states. At $t = 190$ fs, (see Fig. 3(d)) the features of the graphite DOS have developed. The π states now contribute strongly to the DOS, forming the structures on both sides of the Fermi level. These structures show relatively sharp spikes when compared to the DOS of graphite at $T = 0$ K. These result not only from the fact that the newly formed graphite layers are at a high temperature but also reflect the limited number ($N = 216$) of atoms in the MD supercell and thus of the energy levels used to calculate the DOS.

In Fig. 4 we show the DOS that correspond to laser induced ablation of graphite. At $t = 80$ fs (see Fig. 4(b)) the features of the graphite DOS have already significantly broadened, and at the Fermi level the DOS has increased. In Fig. 4(c)) for $t = 160$ fs, the DOS has become metallic-like. The sharp spike close to the Fermi level corresponds to features of the DOS of the linear chain. These features have developed further in Fig. 4(d) for $t = 860$ fs. Note that the state formed during the first 100 fs is a liquid one with low density, due to the expansion of the material. It is a metastable state, since the irradiated region is removed from the system after melting. The short-lived liquid has clear signatures of LDLC [9].

4. Summary

We have presented for the first time calculations of the damage and ablation thresholds in diamond and graphite as a function of the pulse duration in the subpicosecond region. We observe a smooth increase of the thresholds for increasing pulse duration. The order of magnitude of the calculated thresholds are in good agreement with those obtained in experiments.

Acknowledgements

This work has been supported by the Deutsche Forschungsgemeinschaft through SFB 450. A part of the calculations was done on the CRAY T3E at Konrad-Zuse-Zentrum für Informationstechnik Berlin.

References

[1] C.V. Shank, R. Yen, C. Hirlimann, Phys. Rev. Lett. 51 (1983) 900.
[2] D.H. Reitze, H. Ahn, M.C. Downer, Phys. Rev. B 45 (1992) 2677.
[3] P. Stampfli, K.H. Bennemann, Phys. Rev. B 42 (1990) 7163; P. Stampfli, K.H. Bennemann, Phys. Rev. B 49 (1994) 7299.
[4] P. Saeta, J.-K. Wang, Y. Siegal, N. Bloembergen, E. Mazur, Phys. Rev. Lett. 67 (1991) 1023.
[5] D.H. Reize, H. Ahn, M.C. Downer, Phys. Rev. B 45 (1992) 2677.
[6] T. Dallas, M. Holtz, H. Ahn, M.C. Downer, Phys. Rev. B 49 (1994) 796.
[7] H.O. Jeschke, M.E. Garcia, K.H. Bennemann, Phys. Rev. B 60 (1999) R3701.
[8] H.O. Jeschke, M.E. Garcia, K.H. Bennemann, Appl. Phys. A 69 (1999) 49.

[9] H.O. Jeschke, M.E. Garcia, K.H. Bennemann, Phys. Rev. Lett. 87 (2001) 015003.
[10] P.L. Silvestrelli, A. Alavi, M. Parrinello, D. Frenkel, Phys. Rev. Lett. 77 (1996) 3149.
[11] K. Sokolowski-Tinten, J. Solis, J. Bialkowski, J. Siegel, C.N. Afonso, D. von der Linde, Phys. Rev. Lett. 81 (1998) 3679.
[12] S. Preuss, M. Stuke, Appl. Phys. Lett. 67 (1995) 338.
[13] K. Sokolowski-Tinten, J. Bialkowski, D. von der Linde, Phys. Rev. B 51 (1995) 14186and references therein.
[14] K. Sokolowski-Tinten, S. Kudryashov, V. Temnov, J. Bialkowski, M. Boing, D. von der Linde, A. Cavalleri, H.O. Jeschke, M.E. Garcia, K.H. Bennemann, in: Proceedings of the Quantum Electronics and Laser Science Conference, San Francisco, 2000, Tech. Digest 189 (2000); D. von der Linde, K. Sokolowski-Tinten, Appl. Surf. Sci. 154 (2000) 1.
[15] J.S. Horwitz, H.-U. Krebs, K. Murakami, M. Stuke (Eds.), Proceedings of the Fifth International Conference on Laser Ablation, Goettingen 1999, Appl. Phys. A Mater. Sci. Process. 69 (1999) S1–S952.
[16] A.M. Lindenberg, I. Kang, S.L. Johnson, T. Missalla, P.A. Heimann, Z. Chang, J. Larsson, P.H. Bucksbaum, H.C. Kapteyn, H.A. Padmore, R.W. Lee, J.S. Wark, R.W. Falcone, Phys. Rev. Lett. 84 (2000) 111.
[17] M. Lenzner, J. Krüger, S. Sartania, Z. Cheng, Ch. Spielmann, G. Mourou, W. Kautek, F. Krausz, Phys. Rev. Lett. 80 (1998) 4076.
[18] J. Krüger, W. Kautek, Laser Phys. 9 (1999) 30.
[19] B.C. Stuart, M.D. Feit, S. Herman, A.M. Rubenchik, B.W. Shore, M.D. Perry, Phys. Rev. B 53 (1996) 1749.
[20] M. Parrinello, A. Rahman, J. Appl. Phys. 52 (1981) 7182.
[21] C.H. Xu, C.Z. Wang, C.T. Chan, K.M. Ho, J. Phys. Condens. Mat. 4 (1992) 6047.
[22] H.O. Jeschke, M.E. Garcia, K.H. Bennemann, J. Appl. Phys. 91 (2002) 18.
[23] L. Bergmann, C. Schaefer, Optics of Waves and Particles, Walter De Gruyter, Berlin, 1999.